We are IntechOpen,
the world's leading publisher of
Open Access books
Built by scientists, for scientists

4,800
Open access books available

122,000
International authors and editors

135M
Downloads

154
Countries delivered to

Our authors are among the

TOP 1%
most cited scientists

12.2%
Contributors from top 500 universities

CLARIVATE ANALYTICS
BOOK CITATION INDEX
INDEXED

WEB OF SCIENCE™

Selection of our books indexed in the Book Citation Index
in Web of Science™ Core Collection (BKCI)

Interested in publishing with us?
Contact book.department@intechopen.com

Numbers displayed above are based on latest data collected.
For more information visit www.intechopen.com

Tsunami Detection by Ionospheric Sounding: New Tools for Oceanic Monitoring

Giovanni Occhipinti
Institut de Physique du Globe de Paris
France

1. Introduction

After the Great Sumatra Earthquake and the consequent Indian Ocean Tsunami scientific community puts their attention to alternative methods in ocean monitoring to improve the response of the tsunami warning systems.

Improvement of classic techniques, as the seismic source estimation (e.g., Ammon et al., 2006) and densification of number of buoys over the oceans (Gonzalez et al., 2005), was supported by a new effort in remote sensing: nominally the space altimetry observation of the tsunami in the open sea (Okal et al., 1999; Smith et al., 2005) and the tsunami detection by ionospheric monitoring (e.g., Occhipinti et al., 2006). Today the recent tsunamis declare, one times more, the importance to go forward in this direction.

The indirect tsunami observation by ionospheric sounding is based on the idea anticipated in the past by Hines (1972) and Peltier & Hines (1976) that tsunamis produce internal gravity waves (IGWs) in the overlooking atmosphere. During the upward propagation the IGWs are strongly amplified by the effect of the decrease of the density. The interaction of IGWs with the plasma at the ionospheric height produces strongly variation in the plasma velocity and plasma density observable by ionospheric sounding (Figure 1).

This chapter i) resumes the moderne debate based on the Sumatra event (2004) about the tsunami detection by ionospheric sounding to demonstrate the hypothesis anticipated by Peltier & Hines (1976), and identifies the technics that proved and validated it, nominally altimeters and GPS. ii) Supports, with the recent theoretical works, the coupling between the ocean, the neutral atmosphere and the ionospheric plasma during the tsunami propagation and explores, based on the numerical modeling, the remote sensing possibility with additional techniques as the over the horizon radar (OTH-R). iii) Presents the ionospheric observations of the recents tsunamis to prove the systematic detection capability; nominally we review the following tsunamigenic earthquakes: 12 September, 2007, in Sumatra; the 14 November, 2007, in Chile; the 29 September, 2009, in Samoa; and the recent Tohoku-Oki (Japan) earthquake on 11 Mars 2011. We anticipate here that this last event also allow to prove that the signature of tsunami in the ionosphere can be also detected by optical camera *via* the airglow.

It finally concludes discussing the role of ionospheric sounding and remote sensing in the modern evolution of tsunami detection and warning systems.
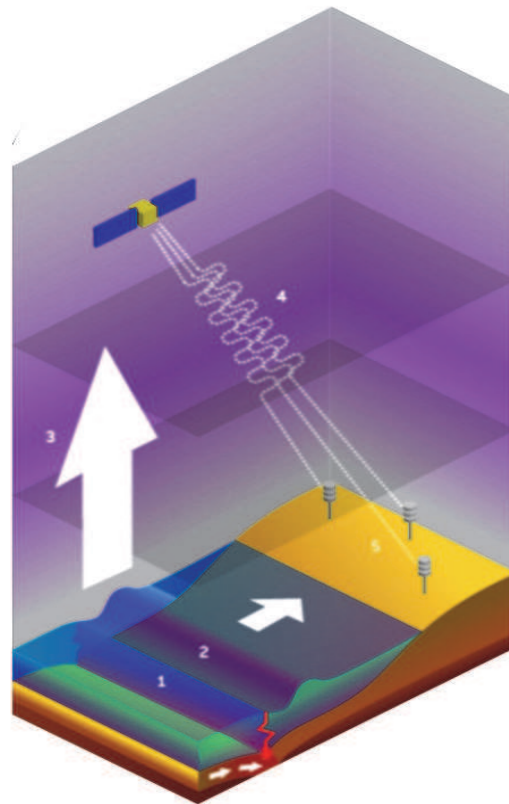
Fig. 1. Schematic view of the coupling mechanism and the ionospheric sounding by GPS. The vertical displacement of the ground floor (1) produced by an earthquake is directly transfered at the sea surface (2) following the incompressible hypothesis. The sea surface displacement initiate an internal gravity wave (IGW) propagating into the ocean (tsunami) as well as into the overlooking atmosphere. During the upward propagation the atmospheric IGW interact with the ionospheric plasma (3) creating perturbation in the plasma density and consequently in the local refraction index. The electromagnetic waves emitted by GPS satellites (4) to the ground stations (5) are perturbed by the plasma density variations and are able to image the signature of the IGW in the ionosphere.

2. The modern debate

The encouraging work of Artru et al. (2005) on the detection of the peruvian tsunamigenic quake on 23 June, 2001 (M=8.4 at 20:33 UT) in the total electron content (TEC) measured by the japanese dense GPS network GEONET opens the modern debate about the feasibility of tsunami detection by ionospheric sounding.

In essence, Artru et al. (2005) shows ionospheric traveling waves reaching the Japanese coast 22 hours after the peruvian tsunamigenic quake, with an azimuth and arrival time consistent with tsunami propagation (Fig. 2). Moreover, a period between 22 and 33 min, consistent with the tsunami, was identified in the observed TEC signals. The tsunami generated internal gravity waves (IGWs) were, however, superimposed by other signals associated with traveling ionospheric disturbances (TIDs) (Balthazor & Moffett, 1997). The ionospheric noise is large in the gravity domain (Garcia et al., 2005), consequently the identification of the tsunami signature in the TEC could be doubtful, and the debate still open.
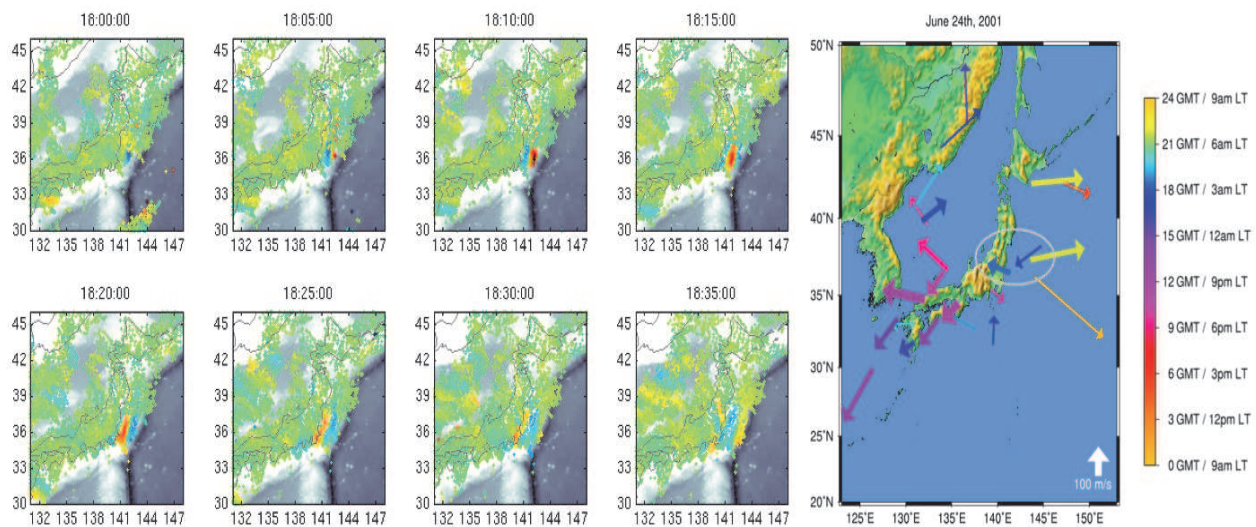
Fig. 2. Left-small-panels: TEC variations plotted at the ionospheric piercing points. A wave-like disturbance is propagating towards the coast of Japan. The perturbation presents characteristics of a tsunami IGW, and arrives approximately at the same time as the tsunami. Right-small-panels: Waves observed on the TEC maps throughout June 24th, 2001. The thickness of the arrows indicate the approximate amplitude of the wave (lower than 0.75 TECU, between 0.75 and 1.5 TECU, and between 1.5 and 2.25 TECU). The direction is the azimuth, and the lenght is proportional to the speed. Finally, the color indicate the time of observation (reddish colors are the local day time, blue is nighttime). The ellipse shows the possible tsunami signal showed in the left-panels. Figure after Artru et al. (2005).

The giant tsunami following the Sumatra-Andaman event (Mw=9.3, 0:58:50 UT, 26 December, 2004 (Lay et al., 2005)), an order of magnitude larger than the Peruvian tsunami, provided worldwide remote sensing observations in the ionosphere, giving the opportunity to explore ionospheric tsunami detection with a vast data set (Fig. 3). In addition to seismic waves detected by global seismic networks (Park et al., 2005); co-seismic displacement measured by GPS (Vigny et al., 2005); oceanic sea surface variations measured by altimetry (Smith et al., 2005); detection of magnetic anomaly (Balasis & Mandea, 2007; Iyemori et al., 2005) and acoustic-gravity waves (Le Pichon et al., 2005); a series of ionospheric disturbances, observed with different techniques, have been reported in the literature (DasGupta et al., 2006; Liu et al., 2006a;b; Lognonné et al., 2006; Occhipinti et al., 2006; 2008b).

Two ionospheric anomalies in the plasma velocities were detected North of the epicenter by a Doppler sounding network in Taiwan (Liu et al., 2006a). The first was triggered by the vertical displacement induced by Rayleigh waves. The second, arriving one hour later with a longer period, is interpreted by Liu *et al.* (2006a) as the response of ionospheric plasma to the atmospheric gravity waves generated at the epicenter.

A similarly long period perturbation, with an amplitude of 4 TECU[1] peak-to-peak, was observed by GPS stations located on the coast of India (DasGupta et al., 2006). These perturbations could be the ionospheric signature of IGWs coupled at sea level with the tsunami or the atmospheric gravity waves generated at the epicenter. Comparable TEC observations were done for five GPS stations (twelve station-satellite couples) scattered in the Indian Ocean (Liu et al., 2006b). The 30 sec differential amplitudes are equal to or smaller than

---

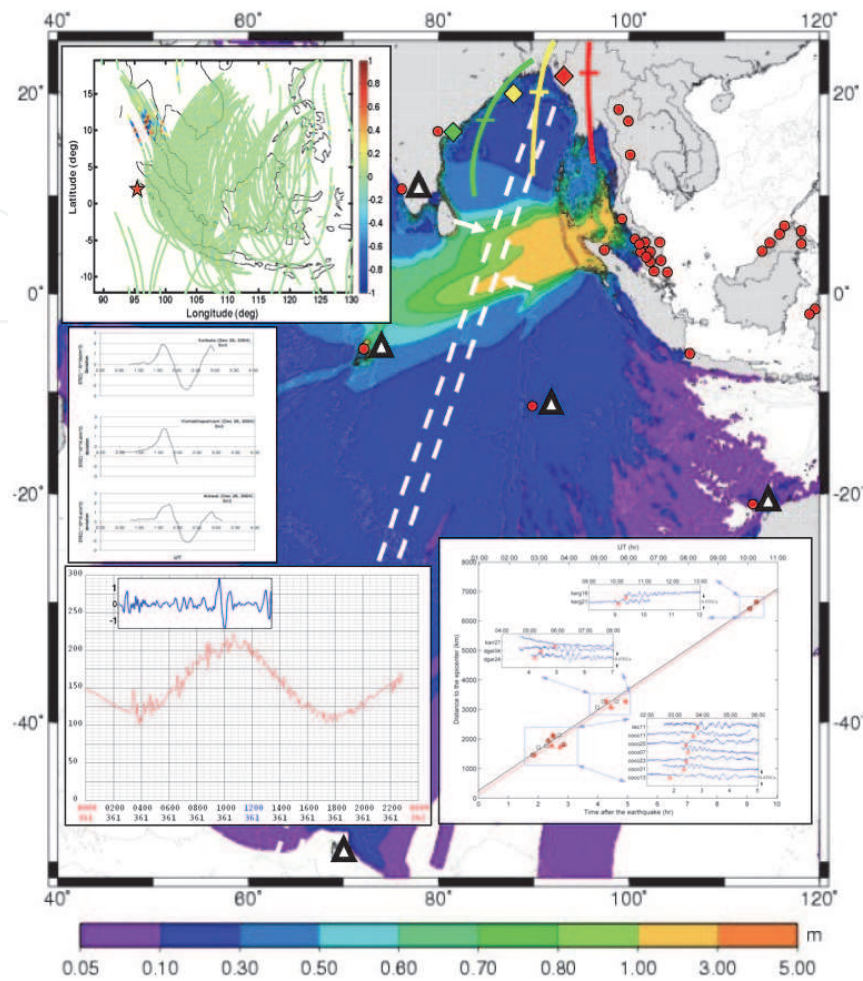[1] The TEC is expressed in TEC units (TECU); 1 TECU = $10^{16} e^- / m^2$.

Fig. 3. Main: Maximum sea-level perturbation model produced by the propagation os the Sumatra tsunami (26 December, 2004). Top: TEC perturbation appearing within 15 min after the tsunami generation. The ionospheric piercing points (IPPs) obtained by satellites PRN01, 03, 13, 19, 20 and 23 coupled with the SEAMARGES network (red point in the main figure) are showed here during 40 min and highlight a clear early perturbation moving from the epicenter (the red star) to the North of Sumatra. Fugure after Occhipinti et al. (2011b). Middle: TEC perturbation observed by DasGupta et al. (2006) with the 3 satellite-station couples showed in the main figure by colored diamonds (station location) and lines (satellites) in the main figure. DasGupta et al. (2006) explain this signal as the IGW generated at the source by the vertical displacement but not link to the tsunami. Bottom-right: Average horizontal speeds of TIDs (red line) and tsunami (black line). The used GPS stations are indicated by triangle in the main figure. Figure after Liu et al. (2006b). Bottom-left: Tsunami signal measured at Coco Island by the tide gauge (red) and by the co-located GPS receiver (blue). The tide gauge measures the sea level displacement (tsunami + tide) and the GPS measures the TEC perturbation in the ionosphere. Both waveforms are similar in showing the sensitivity of ionosphere to the tsunami structure. Figure after Occhipinti et al. (2008b)

0.4 TECU (which generates amplitudes comparable to the DasGupta et al. (2006) observations for periods of $\approx$165 min, *i.e.* 30 points) and the arrival times coherent with the tsunami propagation. The observed satellites were located approximately at the station zenith.

Comparison between oceanic sea-level measured by tide-gauge at Coco Island and the TEC measured by the co-located GPS shows similarity in the waveform suggesting that the ionosphere is sensitive to the tsunami propagation as well as the ocean (Occhipinti et al., 2008b). We highlight that the tsunami reaches Coco Island 3 hours after the tsunami generation, this is the first oceanic observation of the Sumatra tsunami (Titov et al., 2005).

Close to these observations, the Topex/Poseidon and Jason-1 satellites acquired the key observations of the Sumatra tsunami with altimetry profiles. The measured sea level displacement is well explained by tsunami propagation models with realistic bathymetry, and provides useful constraints on source mechanism inversions (e.g. Song *et al.*, 2005). In addition, the inferred TEC data, required to remove the ionospheric effects from the altimetric measurements (Imel, 1994), showed strong anomalies in the integrated electron density (Occhipinti et al., 2006).

In essence, altimetric data from Topex/Poseidon and Jason-1 shows at the same time the tsunami signature on the sea surface and the supposed tsunami signature in the ionosphere (Fig. 4). By a three-dimentional numerical modeling Occhipinti et al. (2006) compute the atmospheric IGWs generated by the Sumatra tsunami and their interaction with the ionospheric plasma. The quantitative approach reproduces the TEC observed by Topex/Poseidon and Jason-1 in the Indian Ocean the 26 December 2004. Consequently, Occhipinti et al. (2006) closed the debate about the nature and the existence of the tsunami signature in the ionosphere. The results obtained by Occhipinti et al. (2006) was recently reproduced by Mai & Kiang (2009).

The TEC observation close to the epicenter using the local GPS network SEAMARGES, shows an early signal appearing at around 20 min after the tsunami generation and observable during 1 hour (Fig. 3). This signal could be contain both, an acoustic-gravity wave perturbation directly link to the vertical displacement at the source, and the tsunami signature in the ionosphere (Occhipinti et al., 2011b). The systematic observation of this early TEC perturbation could be used for tsunami warning system purpose. Anyway, we highlight that today the acoustic-gravity wave signature in the TEC observed close to the epicenter has not been reproduced by modeling.

3. Theoretical works

Tsunamis are long period oceanic gravity waves (Satake, 2002): their frequency is generally much smaller than the atmosheric Brünt-Vaïsalla frequency and, in the limit of linear analysis, they generate internal gravity waves in the overlying atmosphere (Hines, 1972; Lognonné et al., 1998; Occhipinti et al., 2006; 2008a). In other words, the coupling mechanism does not transfer a significant propagating energy in the acoustic domain. As a consequence of this theoretical hypothesis and the slow propagation velocity of IGW, a Bussinesq approximation, equivalent to incompressible fluid (Spiegel & Veronis, 1960), can be used in the ocean-atmosphere coupling mechanism and tsunami-IGW propagation.

Following those hypothesis Occhipinti et al. (2006; 2008a) developed a vertical pseudo-spectral propagator $\frac{dV}{dz} = A \cdot V$ (based on the Navier Stokes equations, the continuity equation and the incompressible hypothesis) explicitly described by the following
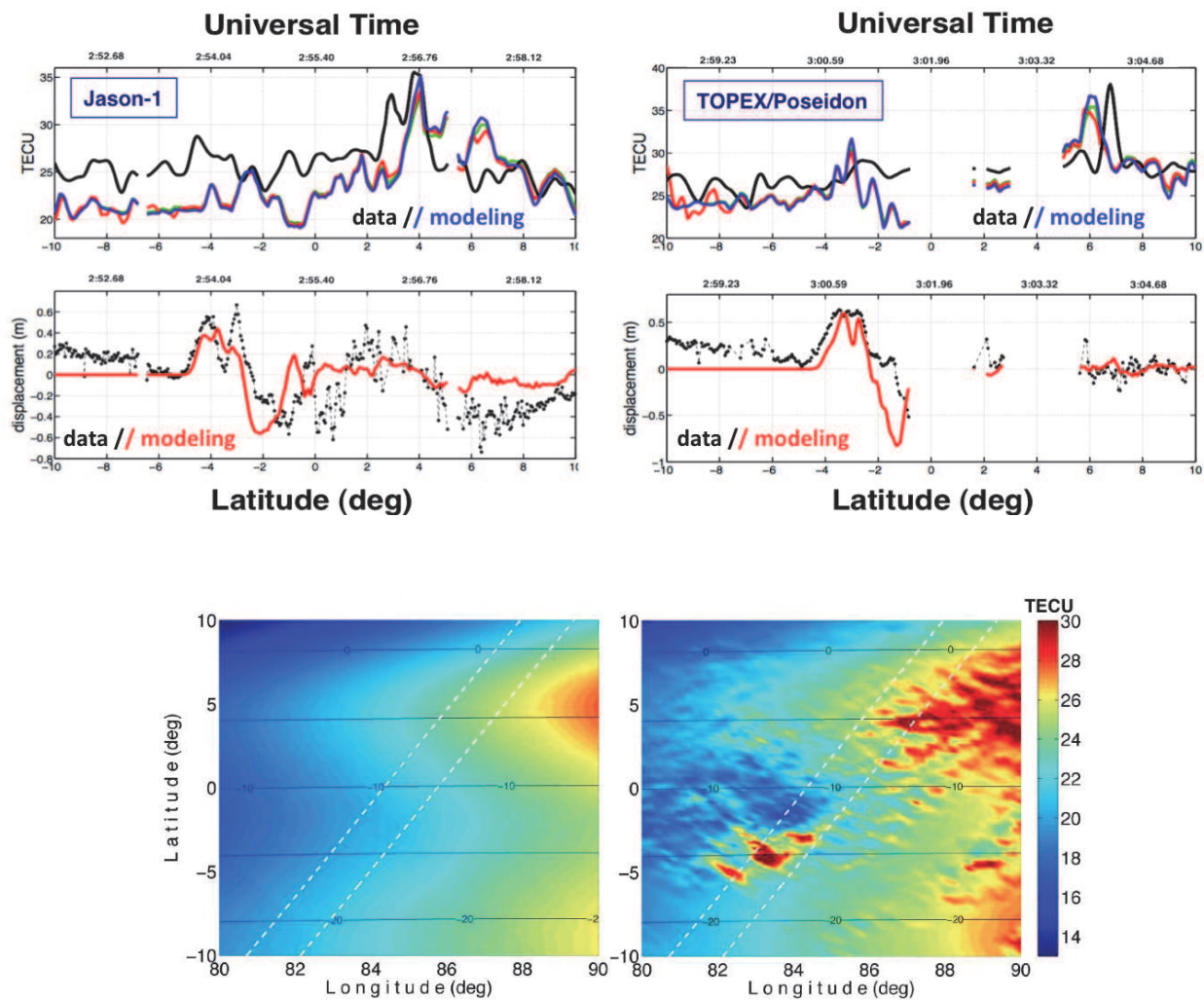
Fig. 4. Top: Altimetric and TEC signatures of the Sumatra tsunami. The modelled and observed TEC are shown for (left) Jason-1 and (right) Topex/Poseidon: synthetic TEC (top-panels) without production-recombination-diffusion effects (blue), with production-recombination (red), and production-recombination-diffusion (green). The Topex/Poseidon synthetic TEC has been shifted up by 2 TEC units. (bottom-panels) The altimetric measurements of the ocean surface (black) are plotted for the Jason-1 and Topex/Poseidon satellites, respectively. The synthetic ocean displacements, used as the source of IGWs in the neutral atmosphere, are shown in red. For each plot from the latitude and corresponding Universal Time are shown. Bottom: Tsunami signature (right) in the TEC at 3:18 UT and (left) the unperturbed TEC. The TEC images have been computed by vertical integration of the perturbed and unperturbed electron density fields. The TEC perturbation induced by tsunami-coupled IGW is superimposed on a broad local-time (sunrise) TEC structure. The broken lines represent the Topex/Poseidon (left) and Jason-1 (right) trajectories. The blue contours represent the magnetic field inclination. Figures after Occhipinti et al. (2006).

vector V and matrix A:

$$V = \begin{pmatrix} \tilde{u}_z^* \\ \tilde{P}^* \end{pmatrix};$$

$$A = \begin{pmatrix} -\frac{1}{\Omega}\left(k_x \frac{du_{x0}}{dz} + k_y \frac{du_{y0}}{dz}\right) & \frac{1}{2}\frac{d\ln\rho_0}{dz} - \frac{i(k_x^2+k_y^2)}{\Omega} \\ i\left(\Omega + \frac{g}{\Omega}\frac{d\ln\rho_0}{dz}\right) & -\frac{1}{2}\frac{d\ln\rho_0}{dz} \end{pmatrix}$$

Where $\tilde{u}_z^* = \sqrt{\rho_0}\,\tilde{u}_z$ and $\tilde{P}^* = \frac{\tilde{P}}{\sqrt{\rho_0}}$ are normalized vertical velocity $\tilde{u}_z$ and pressure $\tilde{P}$ in the *omega-k* domain: in essence the propagating plane waves with horizontal wave-numbers k_x, k_y and angular frequency ω; g is the gravity, ρ_0 is the unperturbed atmospheric density, u_{x0} and u_{y0} are the meridional and zonal background winds, and $\Omega = \omega - u_{x0}k_x - u_{y0}k_y$ is the intrinsic frequency relative to the flow induced by the winds (Nappo, 2002). The effect of the wind on the IGW propagation is fully explored by Sun et al. (2007): in essence the IGW propagating against the wind is amplified, and slow-down compared to the IGW going in the same direction of the wind. This result is corroborated here by figure XX following Occhipinti et al. (2008a).

The methodology entirely described by Occhipinti et al. (2008a) can be simply resumed as follow: the vertical velocity field, induced by the sea motion during the tsunami propagation, is decomposed in planar waves by a three-dimensional Fourier-transform in the Cartesian frame (x, y) and time, where $\hat{x}$ and $\hat{y}$ are eastward and northward. In essence, Occhipinti et al. (2008a) imposes the continuity of vertical displacement between the ocean and the atmosphere. Injected in the propagator described above, it produce the tsunami-related IGW. The other two components of the perturbed velocity $(\tilde{u}_x, \tilde{u}_y)$, and density perturbation $\tilde{\rho}$ are computed from $\tilde{u}_z$ and $\tilde{P}$ as follow:

$$\tilde{u}_x = \frac{1}{\Omega\sqrt{\rho_0}}\left(-i\frac{du_{x0}}{dz}\tilde{u}_z^* + k_x\tilde{P}^*\right)$$

$$\tilde{u}_y = \frac{1}{\Omega\sqrt{\rho_0}}\left(-i\frac{du_{y0}}{dz}\tilde{u}_z^* + k_y\tilde{P}^*\right)$$

$$\tilde{\rho} = \frac{-i}{\Omega\sqrt{\rho_0}}\frac{d\rho_0}{dz}\tilde{u}_z^*$$

Following Occhipinti et al. (2008a; 2011b), in the case of linearized theory for a realistic atmosphere with horizontal stratification and no-background wind, the vertical k-number k_z take the form (1) and consequently the dispersion equation the form (2).

$$k_z = \sqrt{k_h^2\left(\frac{N^2}{\omega^2} - 1\right) - \left(\frac{N^2}{2g}\right)^2} \tag{1}$$

$$\omega^2 = \frac{k_h^2 N^2}{k_z^2 + k_h^2 + \left(\frac{N^2}{2g}\right)^2} \tag{2}$$

Consequently it is possible to evaluate the vertical and horizontal group velocity v_g^z and v_g^h (Fig. 5):
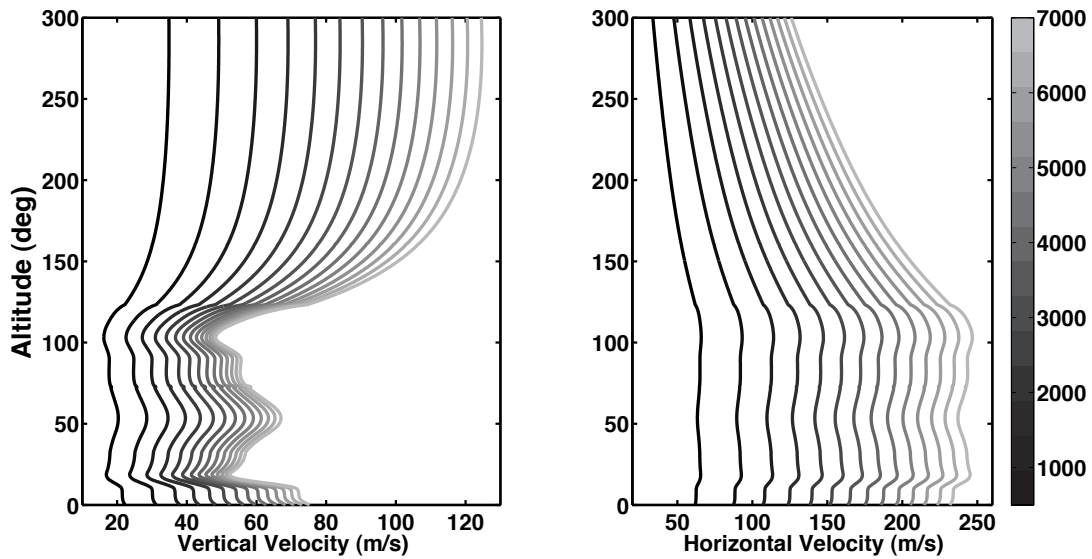
Fig. 5. Vertical (left) and horizontal (right) group velocity of the internal gravity wave coupled at the sea surface with tsunamis (generated at different oceanic deep h, see gray-scale) and a characteristic period T of 10 min. Tsunamis move at the speed defined by the relation $v_{tsuna} = \sqrt{hg}$, where g is the gravity. Consequently, the horizontal k-vector k_h that the tsunami transfer to the atmospheric internal gravity wave also depend by h following the relation $k_h = \frac{2\pi}{T\sqrt{hg}}$. Note that tsunamis generated/moving in the deeper oceanic zone produce faster IGW.

$$v_g^h = \frac{\delta\omega}{\delta k_h} = \frac{k_h N^2 (D - k_h^2)}{\omega D^2} \qquad\qquad v_g^z = \frac{\delta\omega}{\delta k_z} = \frac{k_z k_h^2 N^2}{\omega D^2}$$

where $D = k_z^2 + k_h^2 + \left(\frac{N^2}{2g}\right)^2$ is the denominator of the dispersion equation (2).

The horizontal group velocity don't play a role in the vertical propagation delay but it is useful to estimate the epicentral distance where the internal gravity waves start to interact with the ionosphere as well as the delay between the tsunami propagating at the sea surface and the internal gravity wave propagating in the atmosphere at the ionospheric altitude: *e.g.*, for a period of 10 min, the vertical propagation to reach 300 km is in the order of 1 hour, the horizontal epicentral distance 600 km and the delay between the tsunami and ionospheric IGW wavefronts is in order of 10 min.

The following interaction of IGW with the ionospheric plasma induces perturbation in the plasma density and plasma velocity. In essence, the variation in the neutral velocity $\vec{v}_n$ produced by IGW propagation in the atmosphere produces by dynamic and electromagnetic effect the ions movement with a perturbed speed $\vec{v}_i$ (eq. 4) that induce ion density variation n_i (eq. 3). The principal effect is produced by collisions between the neutral molecules and ions, secondly the ions drag the electrons by charge attraction to satisfy the neutral proprieties of
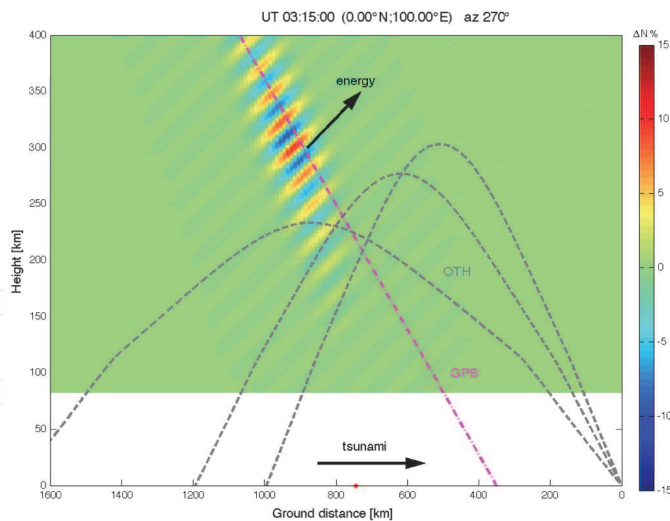
Fig. 6. Vertical cross section of the modeled tsunami-related electron density perturbation and ray-paths computed using a 10 MHz OTH radar signal at 19°, 30° and 35° elevation (dashed gray lines). Dash-dotted purple line indicates a possible geometry of a nearby GPS station for a satellite at 25° elevation. Arrows indicate the tsunami and IGW energy directions of propagation. Note that the vertical scale has been exaggerated. Figure after Coïsson et al. (2011).

the ionosperic plasma (eq. 5).

$$\frac{\partial n_i}{\partial t} + \nabla \cdot (n_i \vec{v}_i) = \pm \beta n_i - \alpha n_i^2 \tag{3}$$

$$\rho_i \frac{d\vec{v}_i}{dt} = -\nabla p_i + \rho_i \vec{g} + n_i q_i (\vec{E} + \vec{v}_i \times \vec{B})$$
$$- \rho_i \mu_{in} (\vec{v}_i - \vec{v}_n) \tag{4}$$

$$n_e = \sum_{i=1}^{3} n_i \tag{5}$$

The method developped by Occhipinti et al. (2006; 2008a) is also used to estimate the role of the geomagnetic field in the tsunami signature at the E-region and F-region (Occhipinti et al., 2008a). Nominally the authors show that the amplification of the electron density perturbation in the ionospheric plasma at the F-region is strongly dependent by geomagnetic inclination as well as by the direction of propagation of the tsunami. This effect is explained by the Lorenz force term in the momentum equation explaining the neutral plasma coupling (eq. 4). Consequently, the detection of tsunamigenic perturbation in the F-region-plasma is easily observed at equatorial and mid-latitude then the hight latitude. The heterogenic amplification drove by the magnetic field is not observable in the E-region, consequently detection at low altitude by Doppler sounding and over-the-horizon (OTH) radar are not affected by geographical location. The theoretical possibility of detection by OTH radar is explored by Coïsson et al. (2011) for a simple tsunami-related IGW (Fig. 6) propagating in an dynamic ionosphere. Coïsson et al. (2011) demonstrate that, in absence of noise, the 3-dimentional pattern of the emission/reception beam of the OTH radar don't hide the tsunami signature (Fig. 7).
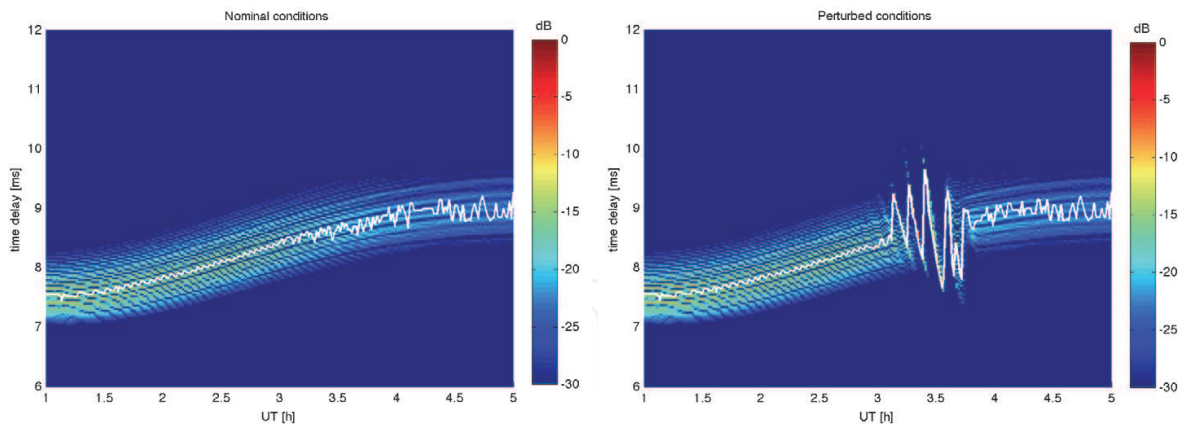
Fig. 7. Synthetic OTH radar record from 01:00 to 0605:00 UT at 270° azimuth 30° elevation during tsunami related IGW propagation showed in Fig. 6. Left: unperturbed ionosphere. Right: ionosphere with IGW perturbation. White points indicate the maximum signal strength at each UT. Figure after Coïsson et al. (2011).
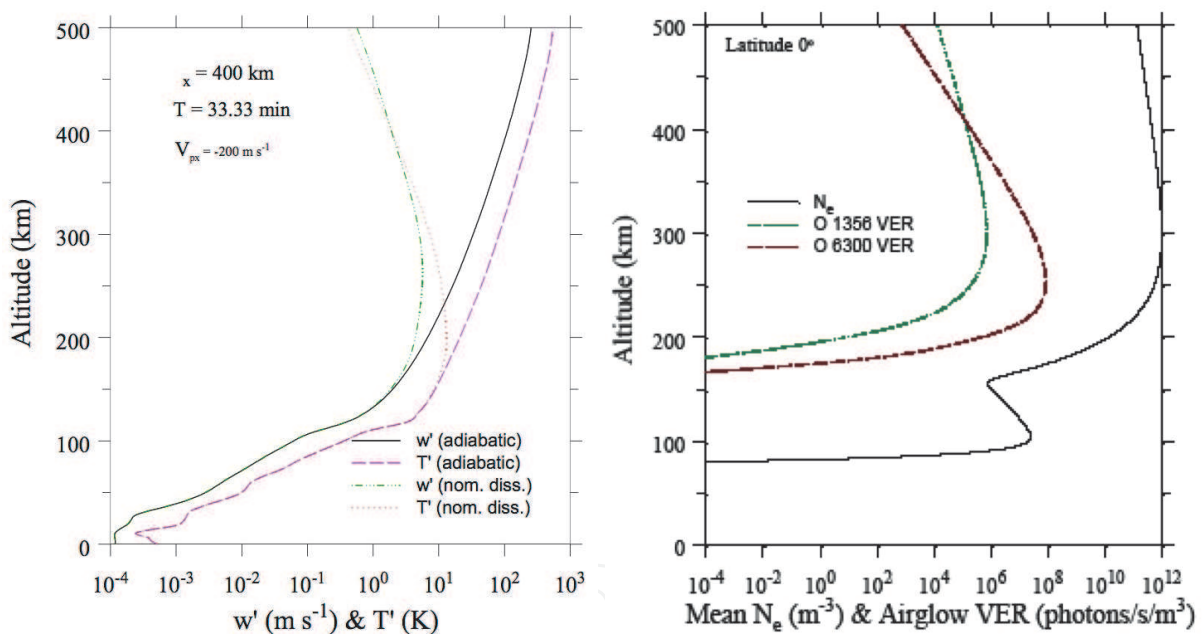

Fig. 8. Left: Relative electron density perturbation induced by tsunami related IGW. Right: Mean electron density (m-3), mean OI 6300 Å VER (photons/s/m3), and mean O 1356 Å VER (photons/s/m3). Figures after Hickey et al. (2009; 2010).

The effect of dissipation, nominally viscosity and thermal conduction have been taken into account in the tsunami atmosphere/ionosphere modeling (Hickey et al., 2009) showing that their effect become non-neglectable above 200 km of altitude (Fig. 8). Consequently, the main theoretical and numerical objective in near future is combine the attenuation effects with a full 3-dimentional modeling.

Theoretical works appeared recently, explore the possible detection by airglow monitoring (Hickey et al., 2010). The recent dramatic event of Tohoku Earthquake (Mw=9.3, 11 March,
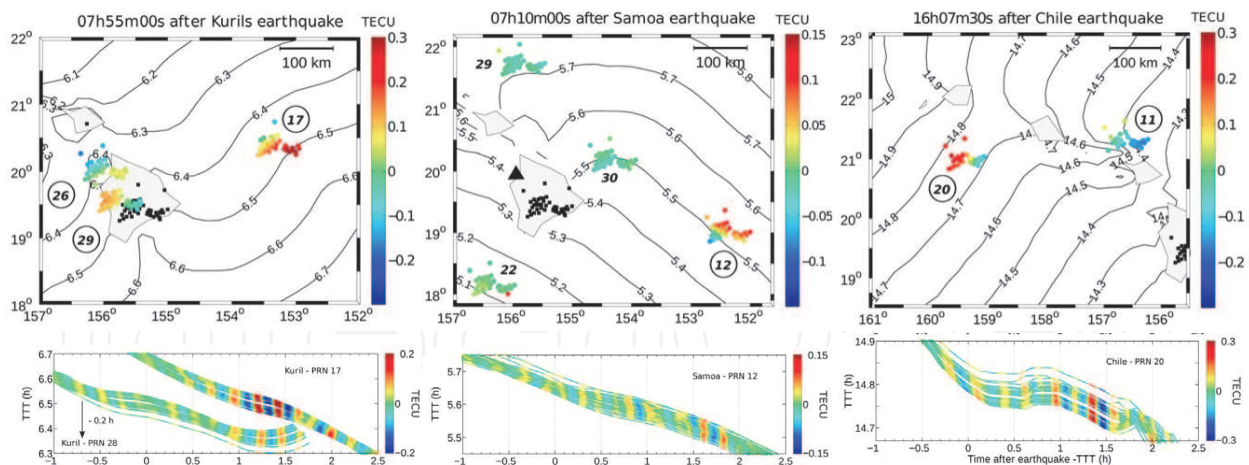
Fig. 9. Top: Instantaneous vTEC plotted about 1 hour after the theoretical tsunami arrival at sea-level, from left to right: after Kuril, Samoa and Chile earthquakes respectively. Bottom: Travel-time diagrams of the vTEC time-series at the time of tsunami arrival off Hawaii, from left to right: for Kuril, Samoa and Chile events, respectively. Time is related to the tsunami travel time to highlight coherence with the tsunami model. Figure after Rolland et al. (2010).

2011, 05:47:32 UT), detailed in the next section, allows to validate this hypothesis comparing measurement and modeling (Makela et al., 2011; Occhipinti et al., 2011a).

4. Recent tsunamis observations

After the ionospheric detection of the great Sumatra earthquake (26 December 2004) and the consequent tsunami, several works focalized on the minor tsunamis in order to generalize and validate the tsunami detection by ionospheric sounding (Galvan et al., 2011; Makela et al., 2011; Occhipinti et al., 2011a; Rolland et al., 2010; 2011).

Rolland et al. (2010) clearly showed the ionospheric detection in the far field for three tsunami events with a moderate magnitude compared to Sumatra: Kuril Islands 2006 (15 November, 2006, Mw 8.3), Samoa 2009 (29 September, 2009, Mw 8.1) and Chile 2010 (27 February 2010, Mw 8.8). Using the Hawaiian GPS network (50 stations) this work highlight the tsunami signature in the TEC. The ionospheric observations, supported by oceanic measurements by DART buoys, showed a signal coherent in arrival time and frequency-signature with the tsunami propagating in the ocean (Fig. 9). Galvan et al. (2011) showed similar coherent observations for Samoa 2009 and Chile 2010 not only in Hawaii but also in Japan, using the dense japanese GPS network GEONET.

Both those studies confirm, one time more, that detection of tsunami by ionospheric sounding is systematic and possible during the propagation in the open ocean.

Close to the epicenter, the coupling mechanism is more complex as the vertical displacement induced by the seismic rupture induces, in the same time, the generation of a propagating acoustic-gravity pulse in the atmosphere (Aframovich et al., 2010; Heki & Ping, 2005; Rolland et al., 2011a) as well as the tsunami formation if the epicenter is in oceanic regions (Occhipinti et al., 2011b). The following tsunami propagation induces, as described above, the formation of gravity wave propagating in the atmosphere and perturbing the ionosphere. Taking into account the theoretical vertical and horizontal speed of tsunami-related IGW (5), Occhipinti et al. (2011b) highlights that the signature of the tsunami with, e.g., a main period of 10 min, in the ionosphere is visible only after 1 hour and at the epicentral distance of 600 km, the
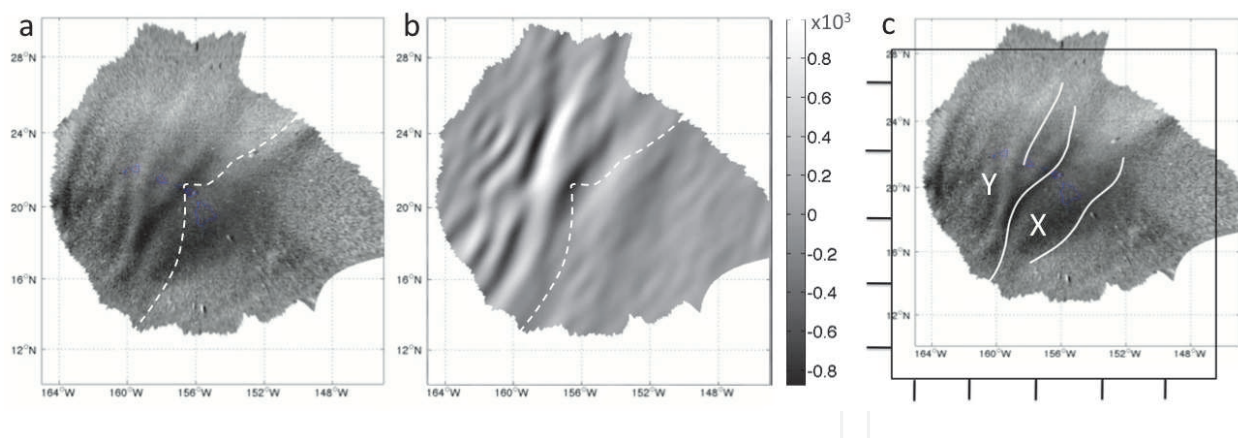
Fig. 10. a) IGW imaged by the 630.0-nm ground-based airglow camera located on the Haleakala Volcano on Maui, Hawaii, at 13:20 UT. b) normalized vertical velocity of the modeled IGW ($(kg/m^3)^{\frac{1}{2}} m/s$). The Y structure as well as the longer wavelength anticipating the Y (X) are present in both, airglow data and AGW synthetics. Those structures are observed between 12:12 to 13:32. The white dotted line in a and b shows the tsunami wavefront line at 13:20 UT. c) graphical estimation of the shift induced by the wind between model and data: the grid and the white lines are estimated on b, then shifted on a to fit with the position of Y and X. The estimated shift of $2°$ is coherent with previous observations Occhipinti et al. (2006). Figure after Occhipinti et al. (2011a).

theoretical estimation is supported by the observation of several tsunamigenic earthquakes: the 26 December, 2004, and 12 September, 2007, in Sumatra; the 14 November, 2007, in Chile; the 29 September, 2009, in Samoa; and the recent Tohoku-Oki (Japan) earthquake on 11 Mars 2011. Additionally, this last work highlight how the sensitivity of the TEC measurement is affected by the inclination angle of the station-satellite line-of-site: as a consequence of the integrated nature of TEC, the low inclination measurements have stronger sensitivity to tsunami signature in the ionosphere.

During the Tohoku-Oki event, close to the TEC measurements by GPS (Rolland et al., 2011) or altimeters (Jason-1), the tsunami related IGW propagating over the Pacific Ocean has also been detected for the first time by the airglow wide-angle camera system located at the top of the Haleakala Volcano on Maui, Hawaii Makela et al. (2011).

In essence, the camera is observing the airglow layer at approximately 250 km in altitude caused by the dissociative recombination of O2+ [Link and Cogger, 1988], which emits photons at 630.0 nm has predicted by Hickey et al. (2010).

Numerical modeling of IGW reproduces the main features observed in the airglow images (Fig. 10) showing interesting likenesses between the model and data, and explaining the nature of the airglow observation (Occhipinti et al., 2011a).

The tsunamic nature of the airglow observation is, first, clearly explained by the presence of a Y shape appearing in both synthetics and data; second, by the presence of a wave with a longer wavelength (indicated by X in Fig. 10) that is arriving before the tsunami front-wave. This observation is theoretically explained by Occhipinti et al. (2011a) as the combined effect of the low bathymetry around Hawaii and the period-dependence of the horizontal IGW speed propagation. In essence, the tsunami related IGW with longer-period go faster than shorter-period, consequently, when the tsunami slow-down by the effect of the low bathymetry close to the Hawaiian arcipelagos, the longer-period IGW goes over the tsunami wavefront.

5. Conclusion and perspectives

The analysis of tsunamigenic ionospheric perturbation observed after major events provides valuable information for understanding the physical processes and explore new techniques for tsunami warning systems. Along this chapter it has shown that early detection of tsunamigenic IGWs is possible using a bunch of remote sensing techniques as the TEC measurement by radar-altimetry and GPS, as well as the observation of the atmospheric airglow.

If the TEC measurement of tsunami seems today an established technique for tsunami observation, it present a large number of limits, primarily the observation geometry, that have to be taken into account for an eventual application in the oceanic monitoring.

The preliminary result about ariglow observation highlights that remote sensing of tsunamis via the atmospheric/ionospheric monitoring by ground-based or on-board camera could be a mature technique for oceanic monitoring and have to find a place in the future of tsunami detection technique.

By numerical modeling recents works prove the ability of additional techniques as the OTH-Radar who measure the perturbation at the ionospheric E-region (around 150 km) reducing, if used close to the epicenter, the response time of detection of the tsunami related IGW.

Anyway resuming, some of this techniques are able to highlight the presence of a tsunami several hours before that the wave hits the coast and could play a revolutionary role of remote sensing in the future tsunami warning systems.

6. Acknowledgments

7. References

Ammon, C. J., A. A. Velasco, T. Lay, Rapid estimation of first-order rupture characteristics for large earthquakes using surface waves: 2004 Sumatra-Andaman earthquake, *Geophys. Res. Lett.*, *33*, L14314, 2006.

Afraimovich, E. L., D. Feng, V. V. Kiryushkin, E. I. Astafyeva, S. Jin, and V. A. Sankov (2010), TEC response to the 2008 Wenchuan earthquake in comparison with other strong earthquakes, *Int. J. Remote Sens.*, 31, 3601–3613, doi:10.1080/01431161003727747.

Artru, J., V. Ducic, H. Kanamori, P. Lognonné, M. Murakami, 2005. Ionospheric detection of gravity waves induced by tsunamis. *J. Geophys. Res.*, 160, 840.

Balasis G. and Mandea M., 2007. Can electromagnetic disturbances related to the recent great earthquakes be detected by satellite magnetometers?, *special issue Mechanical and Electromagnetic Phenomena Accompanying Preseismic Deformation: from Laboratory to Geophysical Scale*, ed. by K. Eftaxias, T. Chelidze and V. Sgrigna, Tectonophysics, 431, doi:10.1016/j.tecto.2006.05.038.

Balthazor, R. L., and R. J. Moffett, 1997. A study of atmospheric gravity waves and travelling ionospheric disturbances at equatorial latitudes, *Ann. Geophysicae*, 15, 1048-1056.

Bilitza, D., 2001. International Reference Ionosphere 2000, *Radio Science*, 36, 2, 261-275.

P. Coïsson, G. Occhipinti, P. Lognonné, L. M. Rolland, Tsunami signature in the ionosphere: the innovative role of OTH radar, *Radio Sci.*, Under Revision, 2011.

DasGupta, A., A. Das, D. Hui, K.K. Bandyopadhyay and M.R. Sivaraman, 2006. Ionospheric perturbation observed by the GPS following the December 26th, 2004 Sumatra-Andaman earthquake, *Earth Planet. Space*, 35, 929-959.

Galvan, D., A. Komjathy, M. P. Hickey, and A. J. Mannucci, The 2009 Samoa and 2010 Chile Tsunamis as Observed in the Ionosphere Using GPS Total Electron Content, J. Geophys. Res., 116, A06318, doi:10.1029/2010JA016204.

Garcia, R., F. Crespon, V. Ducic, P. Lognonné. 3D Ionospheric tomography of post-seismic perturbations produced by Denali earthquake from GPS data. *Geophys. J. Int.*, 163:1049-1064, doi: 10.1111/j.1365-246X.2005.02775.x.

F. I. Gonzalez, E. N. Bernard, C. Meinig, M. C. Eble, H. O. Mofjeld and S. Stalin. The NTHMP Tsunameter Network. *Natural Hazards*, 35: 25–39

Heki, K., and J. Ping, 2005. Directivity and apparent velocity of the coseismic traveling ionospheric disturbances observed with a dense GPS network. *Earth Planet Sci. Lett.*, 236, 3-4, 15, 845-855.

Hickey, M. P., G. Schubert, and R. L. Walterscheid, The Propagation of Tsunami-Driven Gravity Waves into the Thermosphere and Ionosphere, *J. Geophys. Res.*, 114, A08304, doi:10.1029/2009JA014105.

Hickey, M. P., G. Schubert, and R. L. Walterscheid, Atmospheric airglow fluctuations due to a tsunami?driven gravity wave disturbance, *J. Geophys. Res.*, 115, A06308, doi:10.1029/2009JA014977.

Hines, C.O., 1972. Gravity waves in the atmosphere, *Nature*, 239, 73-78.

Imel, D. A., EvaluationoftheTOPEX/POSEIDON dual-frequency ionosphere correction, *J. Geophys. Res.*, 99, 24,895-24,906, 1994.

Iyemori, T., M. Nose, D.S. Han, Y.F. Gao, M. Hashizume, N. Choosakul, H. Shinagawa, Y. Tanaka, M. Utsugi, A. Saito, H. McCreadie, Y. Odagi, F.X. Yang, 2005. Geomagnetic pulsations caused by the Sumatra earthquake on December 26, 2004, *Geophys. Res. Lett.*, 32, L20807.

Lay, T., H. Kanamori, C. J. Ammon, M. Nettles, S. N. Ward, R. C. Aster, S. L. Beck, S. L. Bilek, M. R. Brudzinski, R. Butler, H. R. DeShon, G. Ekstrom, K. Satake, S. Sipkin, 2005. The great Sumatra-Andaman earthquake of 26 December 2004, *Science*, 308, 1127-1133.

Le Pichon, A., P. Herry, P. Mialle, J. Vergoz, N. Brachet, M. Garces, D. Drob, L. Ceranna, 2005. Infrasound associated with 2004-2005 large Sumatra earthquakes and tsunami, *Geophys. Res. Lett.*, 32, L19802.

Liu, J. Y, Y. B. Tsai, S. W. Chen, C. P. Lee, Y. C. Chen, H. Y. Yen, W. Y. Chang and C. Liu, 2006a. Giant ionospheric distrubances excited by the M9.3 Sumatra earthquake of 26 December 2004, *Geophys. Res. Lett.*, 33, L02103.

Liu, J., Y. Tsai, K. Ma, Y. Chen, H. Tsai, C. Lin, M. Kamogawa, and C. Lee, 2006b. Ionospheric GPS total electron content (TEC) disturbances triggered by the 26 December 2004 Indian Ocean tsunami, *J. Geophys. Res.*, 111, A05303.

Lognonné, P., E. Clévédé and H. Kanamori, 1998. Computation of seismograms and atmospheric oscillations by normal-mode summation for a spherical Earth model with realistic atmosphere. *Geophys. J. Int.*, 135, 388-406.

Lognonné , P. J. Artru, R. Garcia, F. Crespon, V. Ducic, E. Jeansou, G. Occhipinti, J. Helbert, G. Moreaux, P.E. Godet, 2006. Ground based GPS imaging of ionospheric post-seismic signal, *Planet. Space. Science*, 54, 528-540.

Makela, J.J., P. Lognonné, H. Hébert, T. Gehrels, L. Rolland, S. Allgeyer, A. Kherani, G. Occhipinti, E. Astafyeva, P. Co?õsson, A. Loevenbruck, E. Clévédé, M.C. Kelley, J.

Lamouroux, Imaging and modelling the ionospheric response to the 11 March 2011 Sendai Tsunami over Hawaii, submitted to *Geophys. Res. Let.*.

Mai, C.-L., and J.-F. Kiang (2009), Modeling of ionospheric perturbation by 2004 Sumatra tsunami, *Radio Sci.*, 44, RS3011, doi:10.1029/2008RS004060.

Nappo, Carmen J., 2002. An Introduction to Atmospheric Gravity Waves. *Int. Geophys. Series*, 85, *Academic Press*.

Occhipinti, G., 2006. Observations multi-paramètres et modélisation de la signature ionosphérique du grand séisme de Sumatra, Ph.D. Thesis, Institut de Physique du Globe de Paris, December 2006, http://www.gps.caltech.edu/~ninto.

Occhipinti, G., P. Lognonné, E. Alam Kherani, H. Hebert, 2006. Three-dimensional waveform modeling of ionospheric signature induced by the 2004 Sumatra tsunami. *Geophys. Res. Lett.*, 33, L20104.

Occhipinti, G., E. Alam Kherani, P. Lognonné, 2008. Geomagnetic dependence of ionospheric disturbances induced by tsunamigenic internal gravity waves. *Geophys. J. Int.*, doi: 10.1111/j.1365-246X.2008.03760.x.

Occhipinti, G., A. Komjathy, P. LognonnÌ', Tsunami detection by GPS: how ionospheric observation might improve the Global Warning System, *GPS World*, 50-56, Feb. 2008

Occhipinti, G., P. Coïsson1, J. J. Makela, S. Allgeyer, A. Kherani, H. Hébert, and P. Lognonné, Three-dimensional numerical modeling of tsunami-related internal gravity waves in the Hawaiian atmosphere, submitted to *Earth Planet. Science*.

Occhipinti, G., L. Rolland, et al., From Sumatra 2004 to Tuhoku-Oki 2011: the systematic GPS detection of the early signature of tsunamigenic internal gravity waves in the ionosphere, *J. Geophys. Res., under submission*

Okal, E. A., A. Piatanesi, P. Heinrich, 1999. Tsunami detection by satellite altimetry, *J. Geophys. Res.*, 104, 599-615.

Park, J., K. Anderson, R. Aster, R. Butler, T. Lay, and D. Simpson, 2005. Global Seismographic Network records the Great Sumatra-Andaman earthquake, *EOS Trans. AGU*, 86(6), 60.

Peltier, W. R., and C. O. Hines, 1976. On the possible detection of tsunamis by a monitoring of the ionosphere. *J. Geophys. Res.*, 81,12.

Rolland, L., G. Occhipinti, P. Lognonné, A. Loevenbruck, The 29 September 2009 Samoan tsunami in the ionosphere detected offshore Hawaii. *Geophys. Res. Lett., 37*, L17191 doi:10.1029/2010GL044479, 2010.

Rolland, L. M., P. LognonnŐ, and H. Munekane, Detection and modeling of Rayleigh wave induced patterns in the ionosphere, *J. Geophys. Res.*, 116, A05320, doi:10.1029/2010JA016060, 2011.

Rolland, L.M., P.LognonnŐ,, E.Astafyeva, E. A. Kherani, N. Kobayashi, M. Mann and H. Munekane, The resonant response of the ionosphere imaged after the 2011Tohoku-Oki earthquake, in press, Earth Planet. Sci., 2011

Satake, K., 2002. Tsunamis, *International Geophysics Series, 81A*, Editors W. H. K. Lee, H. Kanamori, P. C. Jenning and C. Kisslinger, *Academic press*.

Smith, W., R. Scharroo, V. Titov, D. Arcas, and B. Arbic, 2005. Satellite altimeters measure Tsunami, *Oceanography*, 18, 2, 10ï£¡2.

Spiegel, E. A., and Veronis G., 1960. On the Boussinesq approximation for a compressible fluid, *Astrophys. J.*, 131, 442-447.

Sun, L., W. Wan, F. Ding, and T. Mao, 2007. Gravity wave propagation in the realistic atmosphere based on a three-dimensional transfer function model, *Ann. Geophys.*, 25, 1979-1986.

Titov, V., A. B. Rabinovich, H. O. Mofjeld, R. E. Thomson, F. I. González, The global reach of the 26 December 2004 Sumatra tsunami, *Science, 309*, 2045-2048, 2005.

Vigny, C., W. J. F. Simons, S. Abu, R. Bamphenyu, C. Satirapod, N. Choosakul, C. Subarya, A. Socquet, K. Omar, H. Z. Abidin, B. A. C. Ambrosius, 2005. Insight into the 2004 Sumatra-Andaman earthquake from GPS measurement in southeast Asia, *Nature*, 436, 201-206.
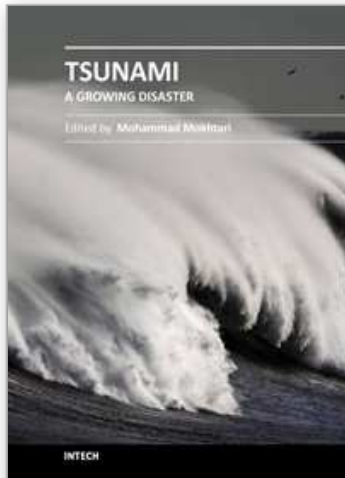
Tsunami - A Growing Disaster

Edited by Prof. Mohammad Mokhtari

ISBN 978-953-307-431-3

Hard cover, 232 pages

Publisher InTech

Published online 16, December, 2011

Published in print edition December, 2011

The objective of this multi-disciplinary book is to provide a collection of expert writing on different aspects of pre- and post- tsunami developments and management techniques. It is intended to be distributed within the scientific community and among the decision makers for tsunami risk reduction. The presented chapters have been thoroughly reviewed and accepted for publication. It presents advanced methods for tsunami measurement using Ocean-bottom pressure sensor, kinematic GPS buoy, satellite altimetry, Paleotsunami, Ionospheric sounding, early warning system, and scenario based numerical modeling. It continues to present case studies from the Northern Caribbean, Makran region and Tamil Nadu coast in India. Furthermore, classifying tsunamis into local, regional and global, their possible impact on the region and its immediate vicinity is highlighted. It also includes the effects of tsunami hazard on the coastal environment and infrastructure (structures, lifelines, water resources, bridges, dykes, etc.); and finally the need for emergency medical response preparedness and the prevention of psychological consequences of the affected survivors has been discussed.

How to reference

In order to correctly reference this scholarly work, feel free to copy and paste the following:

Giovanni Occhipinti (2011). Tsunami Detection by Ionospheric Sounding: New Tools for Oceanic Monitoring, Tsunami - A Growing Disaster, Prof. Mohammad Mokhtari (Ed.), ISBN: 978-953-307-431-3, InTech, Available from: http://www.intechopen.com/books/tsunami-a-growing-disaster/tsunami-detection-by-ionospheric-sounding-new-tools-for-oceanic-monitoring

INTECH
open science | open minds